

533-27

330363
N91-19149

SPACE SIMULATION TEST FOR
THERMAL CONTROL MATERIALS¹

W.R. Hardgrove
TRW Space and Defense Sector

T6013460

ABSTRACT

Tests were run in TRW's Combined Environment Facility to examine the degradation of thermal control materials in a simulated space environment. Thermal control materials selected for the test were those presently being used on spacecraft or predicted to be used within the next few years. The geosynchronous orbit environment was selected as the most interesting. One of the goals was to match degradation of those materials with available flight data. Another aim was to determine if degradation can adequately be determined with accelerated or short term ground tests.

INTRODUCTION

These tests were run in TRW's optical test chamber which is one of three chambers in the Combined Environment Facility (See schematic in Figure 1). This chamber exposes samples to a combined environment of low energy protons, low energy electrons, high energy electrons, near ultraviolet, and far ultraviolet. Thus, synergistic effects of the space environment can be studied. The chamber design permits in situ measurement of solar absorptance so that its degradation can be measured without removal from vacuum.

The nature of thermal control material degradation, being a thin layer or first surface phenomenon, requires a simulation of space radiation environment different from the depth penetration model standards. A radiation survivability analysis has converted the particle population to low energy particles which penetrate thin surface layers. Monte Carlo techniques adapted the low energy particle levels to the potential test materials. Results of the analysis were adjusted to match the capabilities of the facility.

Testing consisted of a battery of three tests. Three different samples of each material were included in the tests for repeatability. The third set of samples was run at a different acceleration rate in an attempt to compare the effects of test acceleration between tests as well as to actual flight data.

1. This work was done under TRW IRAD, "Advanced Thermal Management of Spacecraft," Project No. 88330122, 89330122.

SYMBOLS AND ABBREVIATIONS

Symbols:

A	entrance area to the Faraday cup, $.312 \text{ cm}^2$
α_s	solar absorptance
b	adjustment factor for relative lengths from the source to the sample plane and Faraday cup, .80
I	Faraday cup current
K	charge per proton or electron
n	efficiency of the Faraday cup screen
ϕ	flux desired $\sim p^+/\text{cm}^2 \text{ sec}$ or $e^-/\text{cm}^2 \text{ sec}$

Subscripts:

e	denotes electrons
p	denotes protons

Abbreviations:

CEF	Combined Environment Facility
EUVSH	Equivalent Ultraviolet Sun Hours
FUV	Far Ultraviolet
HEE	High Energy Electrons
LEE	Low Energy Electrons
LEP	Low Energy Protons
NUV	Near Ultraviolet

SELECTION OF MATERIALS

Although many different materials have been run in TRW's combined environment facility, the thrust of this testing was to examine thermal control materials presently used on spacecraft or potentially to be used in near term, i.e., within the next five years. The presently used materials included the usual white paints, i.e., Z93, ZOT, and S13GL0 as well as second surface mirrors. Thermal analysis engineers were polled for other near-term candidates.

Based upon these inputs, seventeen different thermal control materials were selected for study as listed in Table 1. Since the sample plane of the CEF is capable of handling 26 samples and three samples of each material were desired for repeatability, these prospective samples were broken down into two sets as shown in Table 1. The SSM's, which are normally used as contamination monitors during tests of this kind, were used with both sets.

ENVIRONMENTAL PARAMETERS

Since many spacecraft are being designed for geosynchronous orbit, this environment was selected as most interesting. TRW's radiation survivability department was tasked to determine the environment which best matches the CEF capabilities with the radiation environment of geosynchronous orbit. Based upon requirements of present TRW spacecraft and various environmental studies, they were able to determine a fluence profile for a spacecraft in geosynchronous orbit.

With this data and computer techniques which use Monte Carlo methods to establish penetration levels in different materials, analysts modeled the penetration depth of the various types of particles into the materials of interest. Details of the models are discussed in footnote 2. For the analysis, particle levels which were available in the test facility were matched with the same penetration levels as those in the geosynchronous environment.

In this study it was postulated that surface property damage is a function of ionization rather than displacement. With this assumption, a greater number of penetrations through the materials causes a worse degradation of the thermal control surface. Based upon the analysis, the corresponding fluxes which penetrated each thermal surface completely were determined. These fluxes are presented for the first set of samples in Table 2.

Since this test was a multiple sample test, i.e., a test to evaluate more than one type of sample simultaneously, it was necessary to establish a flux to be used on the complement of the samples. Because complete penetration was determined to cause the most damage due to ionization, the maximum fluences on each sample would cause the most damage. Therefore the maximum fluence for each type of radiation would cause the most severe damage for the total. These selected worse or dominating cases are outlined for each particle type in Table 2.

PRE TEST MEASUREMENTS/CALIBRATION

Prior to the test the NUV source was calibrated using a water-cooled, TRW designed, resistor sensor device. This device was attached to the chamber front which places its test plane at the same location as the sample plane. Flux at various settings on the lamp were determined by measuring the resistance change at small openings representing each sample location. This data was read into a computer which with software automatically compares the change between the NUV source and a known source at each location. The same procedure was performed after test shutdown to determine overall NUV fluences during the test sequence.

Normal emittance measurements were made ex situ before and after the test sequence. These values were found by using a Gier-Dunkle Instruments Model DB100 Infrared Reflectometer. Details of the operation of this instrument are described in reference 1.

Ex situ spectral directional reflectance measurements of the samples were made prior to the test using a Beckman DK2A ratio recording spectrophotometer with an integrating sphere attachment of the Edwards type. Details of how these instruments function are discussed in references 2 and 3. These solar absorptance measurements were also made ex situ after completion of the test and removal of the samples from the chamber.

IN SITU MEASUREMENT/CALIBRATION

After the chamber was at vacuum (approximately 1×10^{-6} torr), the solar absorptance of the samples was measured in situ with the Beckman DK2A and repeated periodically during the test sequence to establish the solar absorptance degradation of the sample with time. Next the preliminary calibration of the LEP and LEE was performed. Both sources were calibrated with a Faraday cup which is mounted on an adjustable wand in the chamber. For the pre test calibration the proton source was turned on and adjusted to maintain the required 30 KeV voltage. Then the source was adjusted to maintain the necessary current to give an average flux as desired at the sample plane. Current was measured by a picoammeter and was determined through the characteristics of the Faraday cup in the chamber in relation to the flux by the following equation

$$I_p = \frac{\phi_p A n K_p}{b}$$

A standard nine point calibration was used to describe the average flux over the sample plane. This calibration covers the corners and midpoints. Fluxes at other sample locations were determined by averaging the flux between any two calibration points based upon relative distances to that location.

Calibration of the electron source utilized the same Faraday cup and techniques as described under the proton source calibration. For the pre test calibration, the electron gun was set at the desired voltage of 7 KeV. After the required current was derived from the equation for the desired flux, the electron source was adjusted to project this current on the Faraday cup in front of the center sample in the sample plane. Since the source is angled into the chamber, there is a fall off from left to right over the sample plane. A kill switch on the proton source allows the electron source to be calibrated with the proton source activated.

For the test runs the NUV was set at the maximum current run level at which the pre test calibration was performed. The FUV was set to maximize the energy level at the sample plane. The FUV beam was reflected off a mirror in its path thereby allowing adjustments to direct the beam into its own Faraday cup. Flux at the sample plane was based upon past calibration matches with this current using both an open and an SiO_2 filter condition.

The HEE has a scattering plate in line with the chamber. Current at the plate has been previously calibrated as discussed in reference 4. A current accumulator was used with this previous data to determine when various fluence levels were met.

TEST CONDUCT

Since the proton and low energy flux can be monitored in situ, they were checked periodically utilizing the standard nine point calibration method and adjusted, if necessary, to maintain the required flux levels. For test runs 1 and 2, i.e., sample sets 1 and 2, the samples were exposed for an equivalent of 10 years in geosynchronous orbit. During the tests, in situ spectral reflectance measurements were made at equivalent proton and electron fluence levels to

represent 1, 3, 5, and 10 years of orbital flight. The third test run was a decelerated test which represented 1-1/2 years in orbit. In this test measurements were made at fluences which were equivalent to 3, 6, 12, and 18 months in orbit.

DISCUSSION

The purpose of these tests was to determine if short term ground tests could closely approximate long term, i.e., 5 years or more, degradation of thermal control surfaces. Therefore tests 1 and 2 were accelerated at a high rate to gain the maximum results in the shortest time. For this test series, the maximum acceleration rate was governed by the LEE source. This source was able to provide enough flux to simulate a year of fluence in 72 hours, or an acceleration rate of approximately 120:1. Since both the proton and high energy electrons could provide higher acceleration rates, they were backed down to match the acceleration of the LEE.

Acceleration capability of the solar simulating source was much less than that of the particle sources. The maximum intensity of the NUV varies between 2.0 and 3.0 equivalent suns. The FUV source has no real acceleration capability, i.e., each exposure hour is equivalent to approximately 1 hour in real time. Therefore both the NUV and FUV were run at their maximum levels.

One of the ground test uncertainties in simulating long term degradation is that the acceleration affects the change in properties. Therefore, the third test served as an acceleration effect evaluation by approximating real time exposure rates. This test used the same material types as used in test 1 except that Z93 white paint from set 2 was also included. The final acceleration rate was 2π times the proton and electron levels. This level was chosen to match the NUV acceleration rate of 2 EUVSH and the effects of a rotating spacecraft, i.e., $1/\pi$ suns.

TEST RESULTS

FLUENCES

During the test sequences, current readings at the nine calibration locations were periodically recorded. The readings from the FUV Faraday cup were also recorded at each monitoring time. These data and times were entered along with the pre- and post- test NUV calibrations into a computer program. The program accumulates data during the test sequence and prints out the accumulated fluences of these four sources at any desired time period. Since the high energy electron source uses an accumulator it is integrated in real time and stopped when it reaches the required fluence level. The measured accumulated fluences and the desired levels are compared in Table 3.

PROPERTY DEGRADATION

At any point of interest, when the accumulated flux of the sources was near that desired for that time, the sources were shut down and spectral reflectance

measurements made. In situ spectral measurements were performed by moving each sample from the sample plane into a quartz tube on one side of the vacuum chamber. This test tube fits into the side of an Edward's sphere so that measurements can be made with the attached DK2A. Since the tube introduces some error, these measurements are relative to the initial in situ measurements; i.e., delta changes.

Spectral reflectance data was entered into an HP9000 computer with the aid of an HP9874A. A standard TRW computer program was used to integrate the spectral data over the Thekaekara/NASA solar irradiance curve to determine the solar absorptance, α_s , for each specimen. An HP9872S plotter graphed reflectance curves for each sample.

Spectral reflectance data was used with another TRW-developed program to determine end-of-life properties. This program assumes that solar absorptance degradation is an exponential function. Through a series of curve fitting and cross-referencing at various wavelengths, the program derives an optimum exponential curve fit of the existing data and calculates the maximum solar degradation. Average degradations of the samples are presented in Table 4. Also included in the table are the calculated end-of-life values.

ACCELERATED/DECELERATED TEST COMPARISON

For this parametric evaluation, samples with high degradations were chosen since low degrading samples would match well by definition. Therefore, the most significant changes would appear in the highly degrading samples or, in these tests, ZOT, S13GLO white paint and silvered Teflon. Solar absorptance data from these tests are plotted in Figures 2 through 4 for the three materials. Included with the silvered Teflon data of Figure 4 are results from a previous low rate of acceleration test as discussed in Reference 4.

Data from the two tests for the S13GLO match reasonably well although the lower acceleration environment initially causes a higher degradation in the sample. However, the curve seems to cross over around one year and the high acceleration rate test appears to predict more degradation than the test nearer real time. This condition holds true for both the ZOT and the silvered Teflon as shown in Figures 3 and 4. The ZOT samples actually exhibit a significant deviation between the two tests for the first year to a year and a half. However, the data also appears to cross over at approximately 20 months so that the highly accelerated test data becomes more conservative, i.e., higher degradation.

The silvered Teflon follows the same pattern initially. However, between the 6 month and 9 month measurement there was a significant change in solar absorptance. Originally this was thought to be a measurement problem. But an examination of the samples showed a definite darkening of the sample which would probably cause the deviation in absorptance. At present, the reason for this abrupt change cannot be explained. Interestingly, the 0 to 6 month data seems to project a curve which may line up with the curve for the data from the highly accelerated test.

For comparison purposes, data from a low acceleration test run in 1977 per Reference 4 is included for this sample. Acceleration rates for the test 1977 in were 3π:1. This data shows reasonable agreement with the high acceleration test as run in 1987/1988.

FLIGHT/TEST COMPARISON

Crux of the simulated space test is how its results correlate with actual flight data. Therefore a comparison was made between flight data from three sources and the accelerated simulation test. Data from References 5 and 6 were used as two of the sources for the flight data. The other information includes the most recent property degradation data acquired from TDRSS which is one of TRW's long term satellites.

For this comparison the same three materials were used for the same reason as before, i.e., higher degradation exhibits maximum deviation. Test data for the S13GLO illustrated in Figure 5 shows good agreement with the TDRSS data although it is slightly more conservative. The curve shapes for the test and flight data seem to be the same. Conversely, the ZOT data, as both shown in Figure 6 seems to differ drastically between flight and test. ZOT data from the flight shows very little degradation. For the silvered Teflon as depicted in Figure 7 the test appears to be more conservative than the flight data. There is a good match between the 2 mil samples from the flight and the test sample which, however, was 5 mil.

CONCLUSIONS

Overall the test environment causes a solar absorptance degradation conservatively higher than flight. Nevertheless, the test can be useful in determining if a material will exhibit high degradation in space. Therefore, samples of new materials can be evaluated by short term acceleration simulations. However, for accurate data on a candidate material a limited acceleration is in order.

One interesting note from the tests is that the S13GLO data shows the match between flight and test data. Also, the S13GLO test and flight proton dosages matched best. Since there is conjecture that protons are the most damaging environmental component for materials of this type, perhaps a better proton match for other materials would exhibit correspondingly better correlation.

In conclusion, these tests indicated that an accelerated combined environment simulation may be used to evaluate thermal control materials which exhibit a high degradation in space or are stable. Further, the tests are generally conservative so that this data can be used for "worst case" analyses. Possibly, with a better environmental match and minimum allowable acceleration times, accurate end-of-life properties extrapolations can be obtained.

REFERENCES

1. K.E. Nelson and E.E. Luedke, and J.T. Bevans, "A Device for the Rapid Measurement of Total Emittance," J. Spacecraft Rockets 3:758-760 (1966).
2. L. Cahn and B.D. Henderson, "Performance of the Beckman DK Spectrophotometer," J.O.S.A. 48:380-387.
3. D.K. Edwards, et al, "Integrating Sphere for Imperfectly Diffuse Samples," J.O.S.A. 51:1279-1288 (1961).
4. "Properties of Metallized Flexible Materials in the Space Environment Final Report," TRW 26177-6048-RU-00/SAMSO TR78-31, Contract F04701-74-C-0562 Seq. No. A002, January 1978.
5. D.F. Hall and A.A. Foote, "Long-Term Performance of Thermal Control Coatings at Geosynchronous Altitude," AIAA-86-1356, AIAA/ASME 4th Thermophysics and Heat Transfer Conference, Boston, MA, June 1986.
6. C.C. Anderson and M.M. Hattar, "Calorimetric Measurements of Thermal Control Surfaces at Geosynchronous Orbit," Journal of Thermophysics and Heat Transfer, Volume 2, April 1988, pp. 145-151.

Set 1

Sample Type	Thickness	
	Cm	(In)
1) Second Surface Quartz Mirror	.015-.020	(.006-.008)
2) Silvered Teflon	.019	(.0085)
3) ZOT White Paint	.013-.020	(.005-.008)
4) S13G White Paint (with new binder)	.013-.020	(.005-.008)
5) Astroquartz	.023	(.009)
6) Aluminized Kapton, Sputtered ITO Overcoat	.003	(.001)
7) Leafing Aluminum Paint	.003-.005	(.001-.002)
8) Fibrous Reinforced Composite Insulation (FRCI)	.508	(.200)

Set 2

Sample Type	Thickness	
	Cm	(In)
1) Second Surface Quartz Mirror	.015-.020	(.006-.008)
2) Black Kapton	.005	(.002)
3) Z-93 White Paint	.013-.020	(.005-.008)
4) Chem Filmed Aluminum	- - - - -	- - - - -
5) FRCI-II	.508	(.200)
6) Beta Cloth	.020	(.008)
7) White Chem-Glazed Paint	.013-.020	(.005-.008)
8) Expanded Teflon on Kapton	.013/.005/.003	(.005/.002/.001)
9) VDA on Coated Aluminum	1000A	

Table 1 Spacecraft Thermal Control Materials

Sample	30 KeV Proton $\phi(p/cm^2)$	7 KeV Electron $\phi(e/cm^2)$	800 KeV Electron $\phi(e/cm^2)$
1) Second Surface Quartz Mirror	3.57×10^{16}	6.02×10^{16}	1.88×10^{16}
2) Silvered Teflon	3.35×10^{16}	6.74×10^{16}	3.58×10^{16}
3) ZOT White Paint	2.92×10^{16}	9.03×10^{16}	1.73×10^{16}
4) S13G White Paint	4.02×10^{16}	4.98×10^{16}	1.85×10^{16}
5) Astroquartz	3.55×10^{16}	7.07×10^{16}	1.93×10^{16}
6) Aluminized Kapton-Sputtered ITO Overcoat	1.42×10^{16}	1.08×10^{17}	4.10×10^{16}
7) Leafing Aluminum Paint	3.09×10^{16}	8.40×10^{16}	1.71×10^{16}
8) FRCI	3.86×10^{16}	5.64×10^{16}	1.88×10^{16}

**Table 2 Recommended Test Particle Fluences for Simulation
of 10 Years on Geosynchronous Environment**

Source	Goal	Actuals	
		Set 1	Set 2
30 keV Protons	4.02×10^{16} p/cm ²	6.64×10^{16} p/cm ^{2**}	7.31×10^{16} p/cm ^{2**}
7 keV Electrons	1.08×10^{17} e/cm ²	1.11×10^{17} p/cm ^{2**}	7.49×10^{16} e/cm ^{2**}
800 keV Electrons	4.10×10^{16} e/cm ²	- - - - -	4.10×10^{16} e/cm ^{2**}
NUV	27884 EUVSH*	2290 EUVSH	1900 EUVSH
FUV	27884 EUVSH*	1073 EUVSH	1651 EUVSH

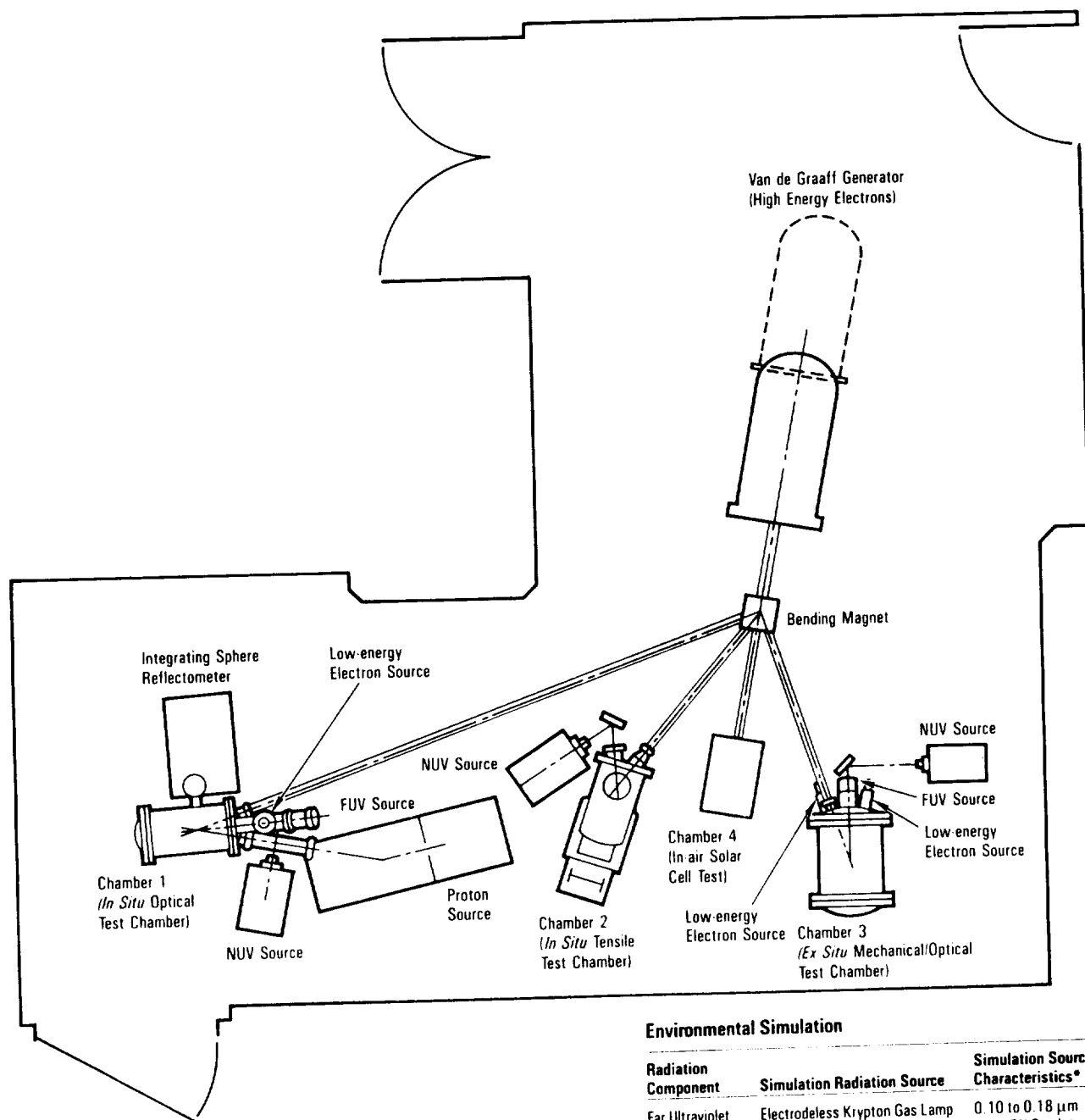
* NUV and FUV requirements are for a spinning or earth-oriented spacecraft (orbit time/ π) These sources are run at maximum levels during the accelerated test. NUV values are averages over the sample plane while FUV values are maximums.

** Protons and electron fluences are average values over the sample plane.

Table 3 10-year Equivalent Test Fluences

	Solar Absorptance After Time in Orbit (Years)					∞ (extrapo- lated)	Hemispherical Emittance After Time in Orbit	
	0	1	3	5	10		0	10
Set 1								
1) Silvered Teflon	0.09	0.13	0.19	0.22	0.25	0.27	0.78	0.78
2) ZOT White Paint	0.15	0.40	0.55	0.62	0.65	0.65	0.85	0.85
3) S13G/LO White Paint (with new binder)	0.26	0.56	0.62	0.68	0.71	0.71	0.86	0.81
4) Astroquartz	0.32	0.38	0.44	0.47	0.50	0.51	0.83	0.83
5) Aluminized Kapton, Sputtered ITO Overcoat	0.38	0.38	0.39	0.39	0.40	0.40	0.12	0.12
6) Leafing Aluminum Paint	0.30	0.32	0.34	0.34	0.35	0.36	0.31	0.29
7) FRCI	0.22	0.31	0.31	0.31	0.37	0.37	0.84	0.84
Set 2								
1) Black Kapton	0.93	0.92	0.92	0.92	0.91	0.89	0.77	0.77
2) Z93 White Paint	0.19	0.28	0.38	0.45	0.52	0.52	0.87	0.85
3) Chem Filmed Aluminum	0.41	0.37	0.37	0.38	0.41	0.41	0.06	0.06
4) FRCI-II	0.23	0.27	0.25	0.27	0.32	0.47	0.84	0.84
5) Beta Cloth	0.30	0.47	0.50	0.54	0.59	0.59	0.86	0.86
6) White Chem Glaze Paint	0.29	0.68	0.71	0.74	0.77	0.77	0.85	0.83
7) Expanded Teflon on Kapton	0.18	0.37	0.46	0.60	0.62	0.65	0.68	0.68
8) VDA on Coated Aluminum	0.10	0.12	0.13	0.14	0.14	0.14	0.02	0.06

Table 4 Average Thermal Control Material Degradation in Simulated Geosynchronous Orbit



Environmental Simulation

Radiation Component	Simulation Radiation Source	Simulation Source Characteristics*
Far Ultraviolet	Electrodeless Krypton Gas Lamp	0.10 to 0.18 μm Up to 5X Sun Intensity
Near Ultraviolet	3-kW Short-arc Xenon Lamp	0.18 to 0.40 μm Up to 3X Sun Intensity
Radiation Belt Electrons	Van de Graaff Accelerator	70 keV to 1.1 MeV 10^7 to 10^{12} $\text{e}/\text{cm}^2\text{sec}$
Plasma Sheet Electrons	Electron Flood Gun	0.5 to 10 keV Up to 10^{11} $\text{e}/\text{cm}^2\text{sec}$
Radiation Belt Protons	Ionization Equivalent Electrons from Van de Graaff Accelerator	70 keV to 1.1 MeV 10^7 to 10^{12} $\text{e}/\text{cm}^2\text{sec}$
Solar Flare Protons	Ionization Equivalent Electrons from Van de Graaff Accelerator	70 keV to 1.1 MeV 10^7 to 10^{12} $\text{e}/\text{cm}^2\text{sec}$
Plasma Sheet Protons	Hydrogen-ion Plasma Generator	Up to 30 keV Up to 10^{12} $\text{p}/\text{cm}^2\text{sec}$
Vacuum	GN_2 Aspiration, Cryosorption, and 400 l/sec Ion Pumping	10^{-6} to 10^{-8} torr

*Radiation zone at the target plane is ≈ 15 cm (6 in) diameter.

Figure 1. CEF Schematic

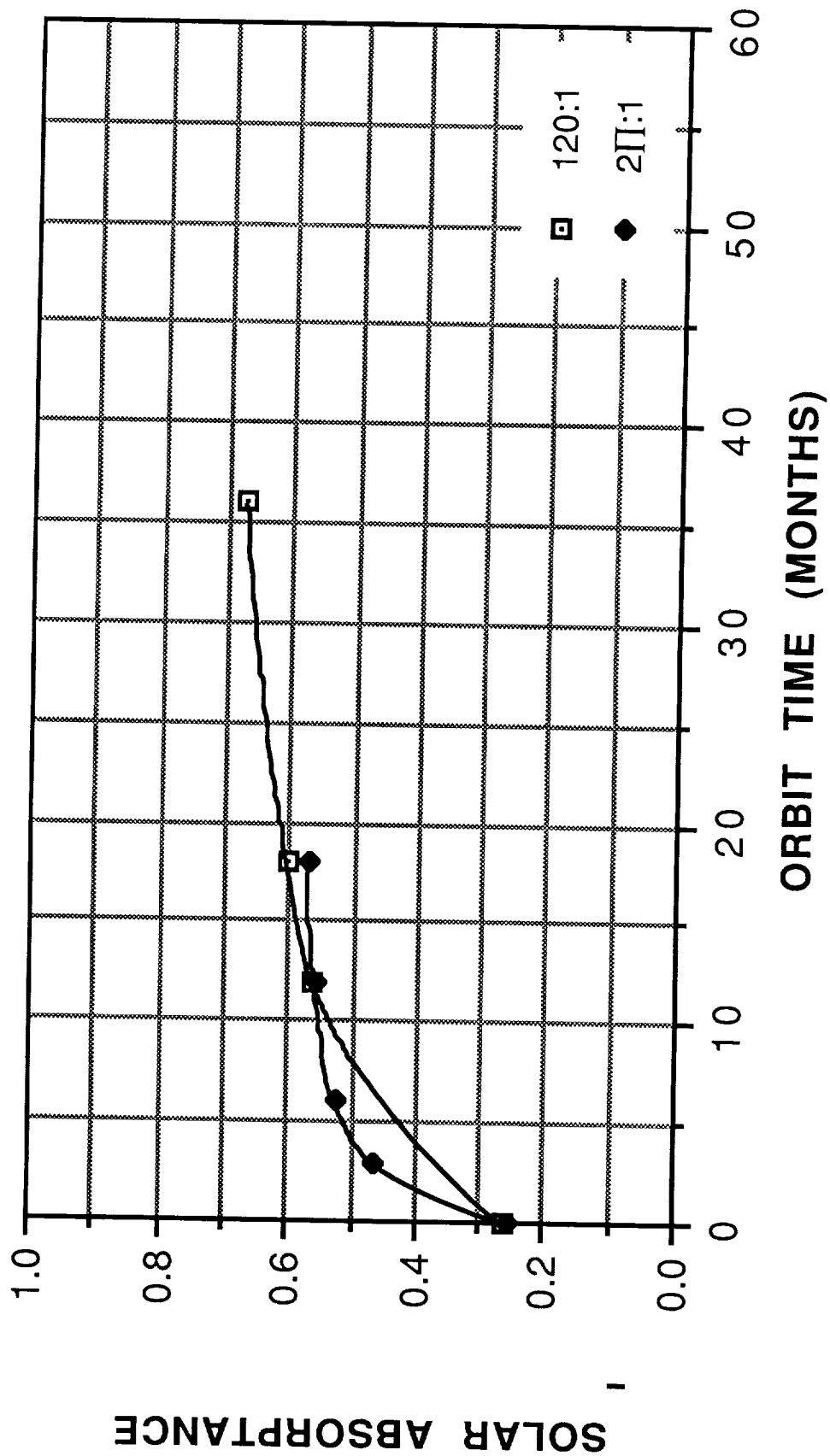


Figure 2. Comparison of Solar Absorbance Degradation of S13G-LO Paint for High and Low Accelerated Simulated Environmental Tests

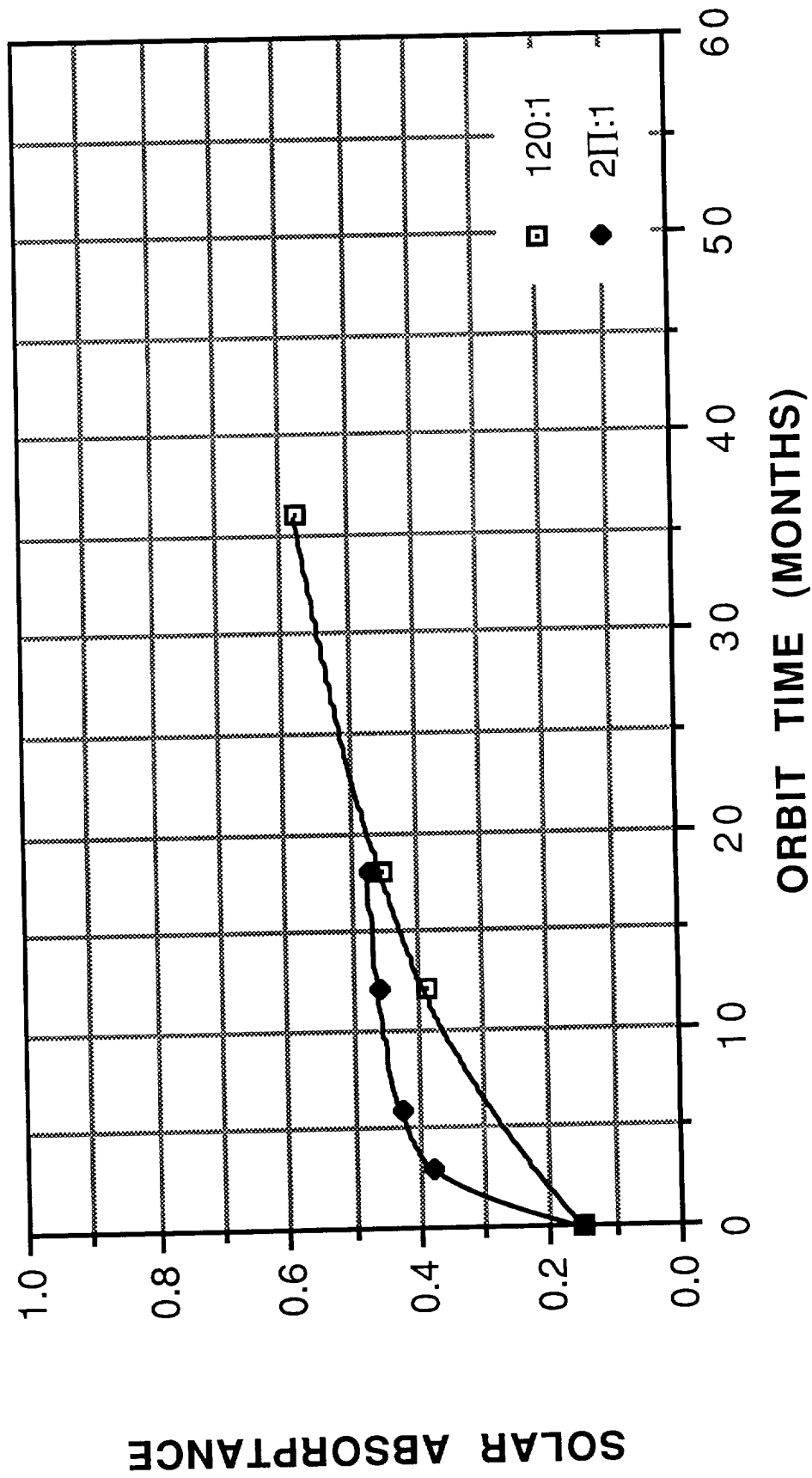


Figure 3. Comparison of Solar Absorptance Degradation of ZOT Paint for High and Low Accelerated Simulated Environmental Tests

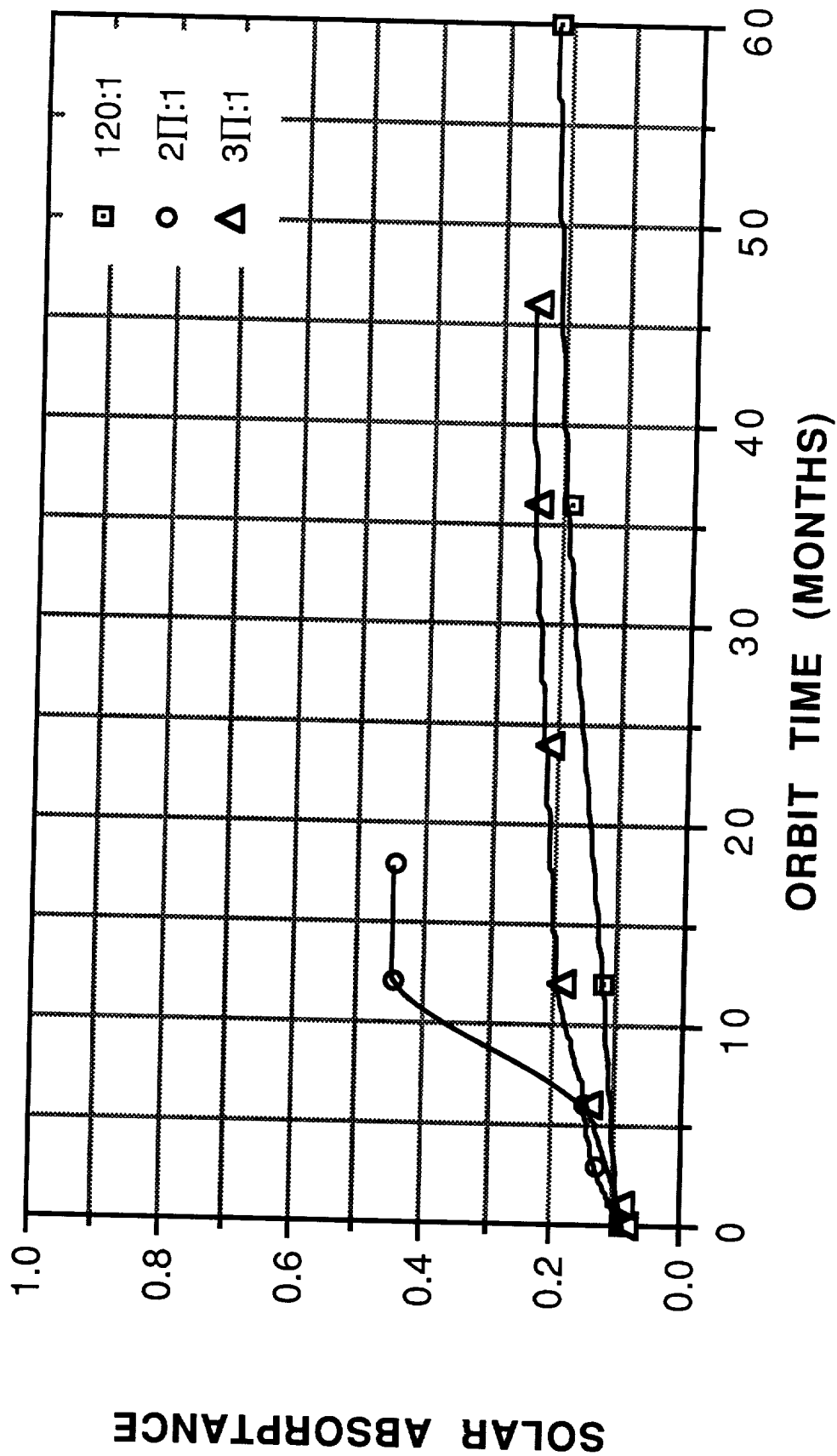


Figure 4. Comparison of Solar Absorbance Degradation of Silvered Teflon for High and Low Accelerated Simulated Environmental Tests

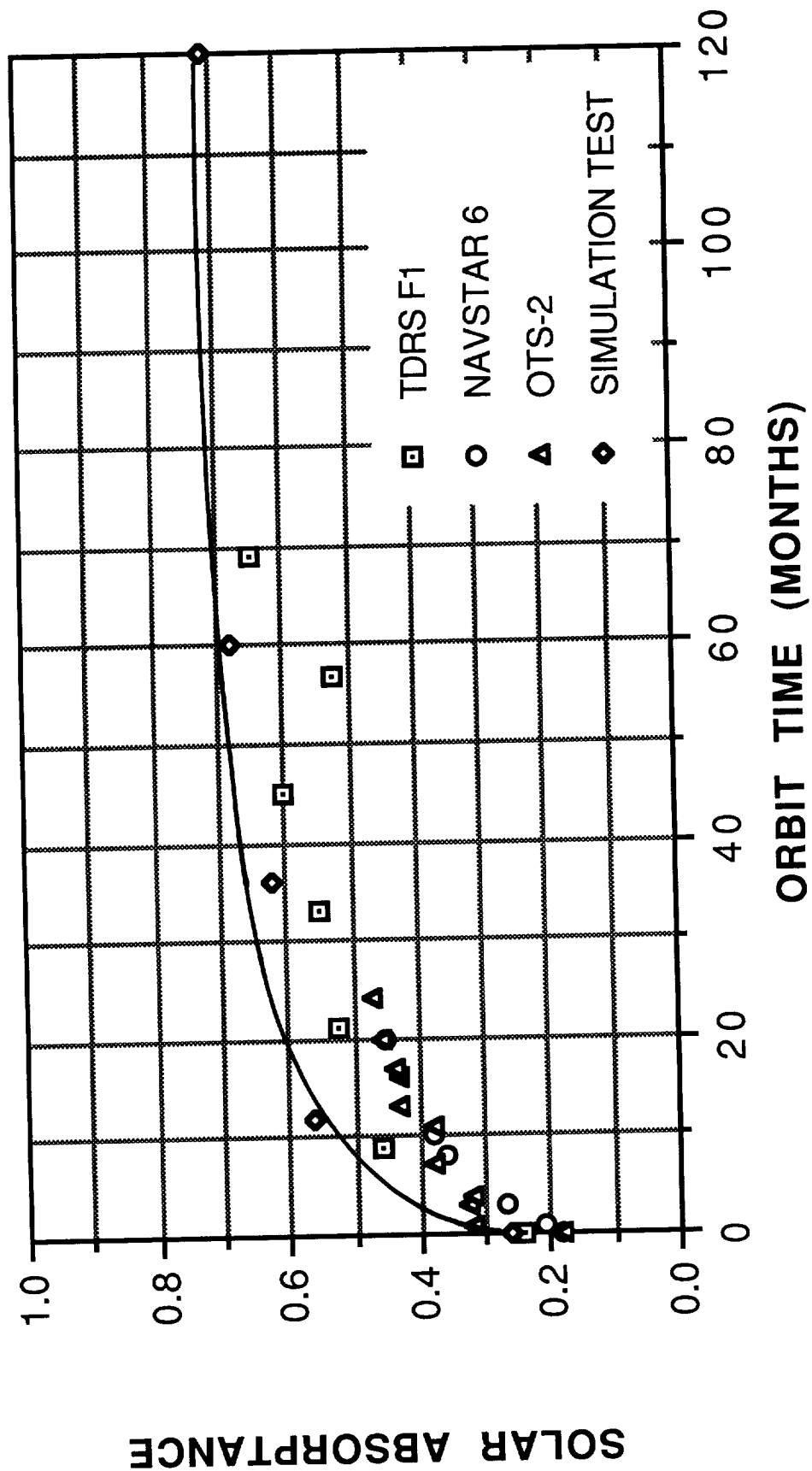


Figure 5. Comparison of Solar Absorbance Degradation for S13G-LO Paint for Simulation Test vs. Flight Data

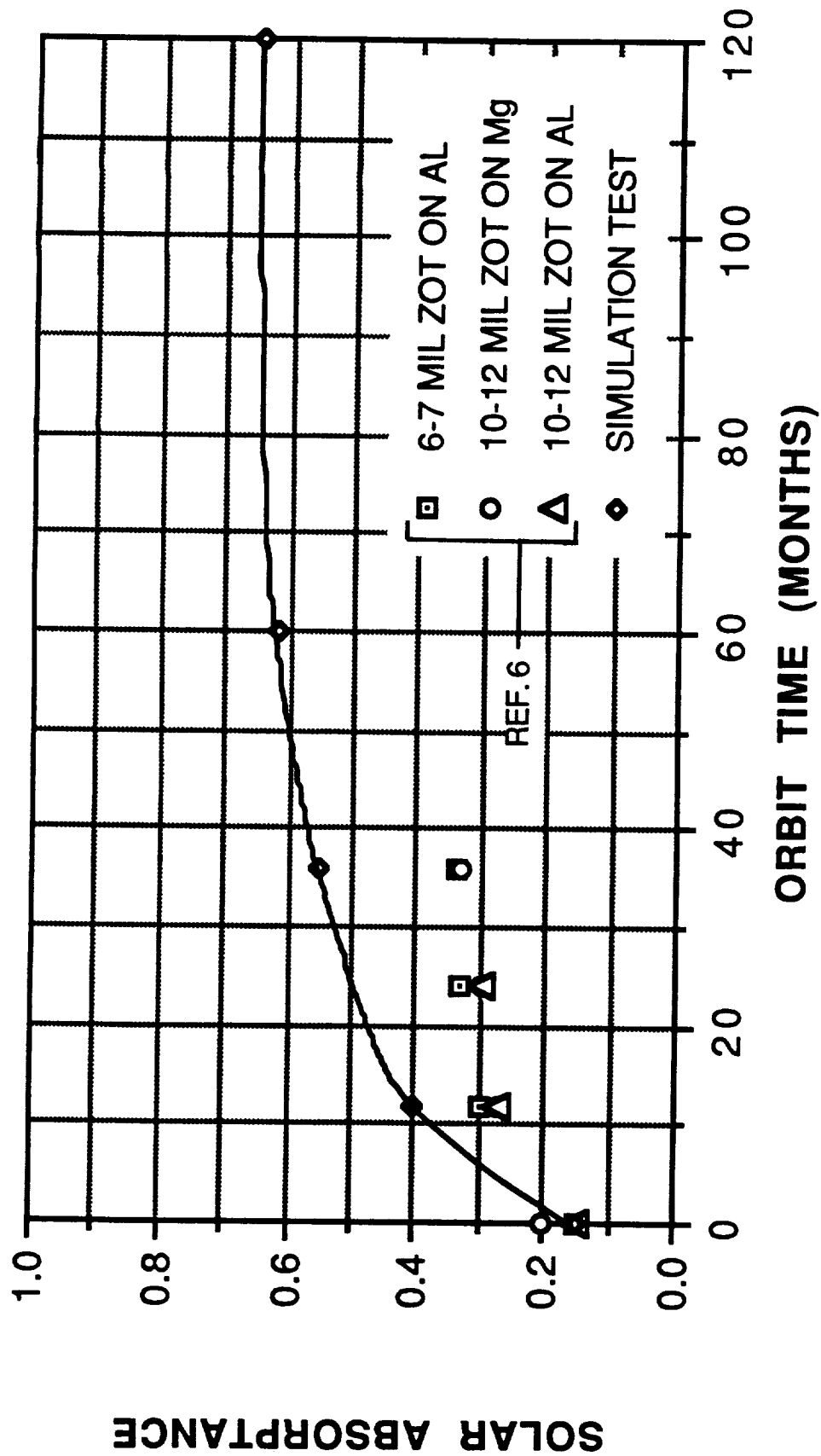


Figure 6. Comparison of Solar Absorptance Degradation for ZOT Paint for Simulation Test vs. Flight Data

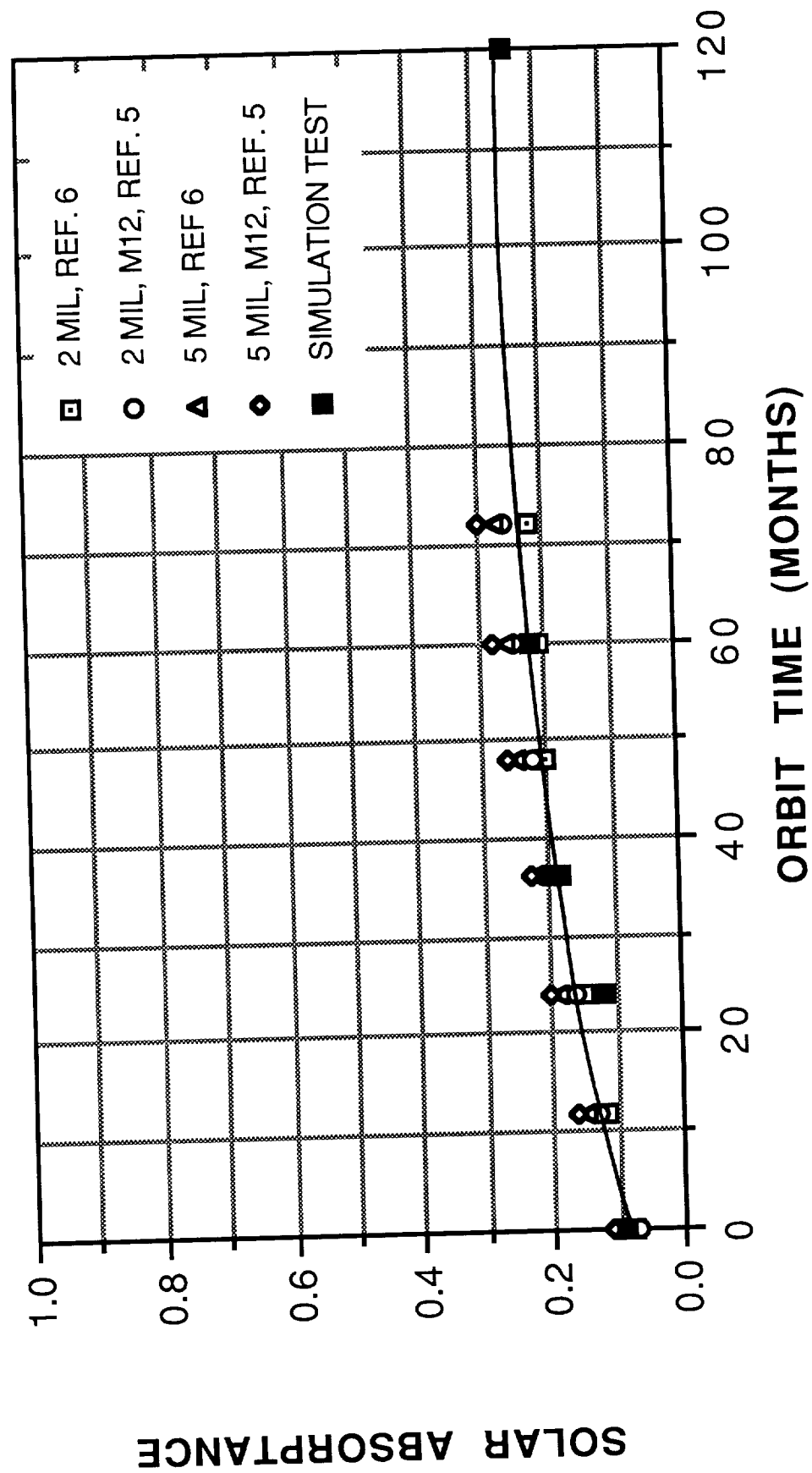


Figure 7. Comparison of Solar Absorptance Degradation for Silvered Teflon for Simulation Test vs. Flight Data

SESSION VII

FACILITIES

